Siddiqui, Tauseef Ahmad; Holopainen, Jari; Viikari, Ville

Beam-Steerable Transponder Based on Antenna Array and Phased Modulators

Published in:
IEEE Antennas and Wireless Propagation Letters

DOI:
10.1109/LAWP.2021.3049972

Published: 01/03/2021

Document Version
Publisher's PDF, also known as Version of record

Beam-Steerable Transponder Based on Antenna Array and Phased Modulators

Tauseef Ahmad Siddiqui, Jari Holopainen, and Ville Viikari, *Senior Member, IEEE*

***Abstract*—This letter presents a novel concept of beam-steerable transponder based on antenna array and phased modulators. The steerability of the beam is achieved by optimally delaying the modulated reflected signal at each antenna element (i.e., changing the phase in frequency domain) with load modulation technique. In this manner, the reflected backscattered signal power can be maximized at one particular direction. The approach makes transponder to collect ambient waves from any direction and further modulate and redirect it to any other direction. The results obtained through experimentation proves the feasibility of omnidirectional transponder and pave way for future lower power smart devices. The transponder functions in the Wi-Fi frequency band of 2.4 GHz.**

***Index Terms*—Ambient signals, antenna array, backscatter, beam steering, Internet of Things (IoT), load modulation, rescatter, retrodirectivity, WSNs.**

I. Introduction

MODULATED backscatter method has rapidly become modus operandi for low-power wireless communication systems [Internet of Things, wireless sensor networks (WSNs)]. Ambient backscatter communication systems (ABCSs) use already available RF sources, e.g., TV towers, FM broadcasting stations, cellular base stations, and Wi-Fi access points for their operations [1]–[3]. The RF sources in ABCSs are unpredictable regarding transmission powers and locations. Therefore, effective use of RF sources require the transponder to tune its operation, where the highest ambient power is available. In our proposed approach, we can have a transponder that receives the ambient RF wave from any direction and further modulates and redirects it to any other direction depending on the backscatter receiver position. The traditional transponders are either almost isotropic or rely on retrodirectivity. Isotropic transponders receive signals from all directions almost equally well and also spreads the rescattered energy evenly across the sphere. The benefit of this approach is its simplicity. However, it utilizes the available RF power less than optimally, because of very low antenna gains both in reception and transmission, resulting into small modulated scattering sections of the transponders.

The previous literature has introduced methods to maximize backscattered power in monostatic case for instance by using the well-known Van Atta array [4] and PON array [5]. However, they are less common in low-power applications due to power hungry components [6], [7]. In another approach, coupler-based retrodirective sensors are presented but these techniques are limited to two-antenna elements [8], [9]. RF circulators [10] and analog circuits [11] can be used to improve the backscattered received power but these devices add complexity and losses in the system. The initial ideas of beam-steerable transponders are introduced in our previous work [12]. This letter presents the theoretical formulation of the concept based on the theory of antenna arrays and extends to bistatic transponders. We have previously described how a transponder based on multiple-phased modulators can be made frequency reconfigurable [13], [14]. The transponder is equipped with multiple, mutually coupled antenna elements, each terminated with independently controlled modulators. The operation frequency of the transponder is reconfigured by changing the phase delays of the modulators.

In this letter, we use similar kind of multiload modulation method to realize a transponder whose receive and transmit beams can be controlled separately by adjusting modulator delays. We explain the operation principle with an analytical model and experimentally demonstrate the concept with a novel transponder designed for the purpose.

II. Theoretical Construction

A. Load Modulation

In backscatter communication systems, a binary (two-state) load modulation is used for simplicity. In general, the transponder modulates both the amplitude and the phase of the scattered signal. To arise the phase modulation only, the reflection coefficient at each load ($\rho_{\text{load}1,\ldots,N}$) can be shifted between absorbing and reflecting states by switching between two loads $Z = 0$ and $Z = \infty$, as shown in Fig. 1. This leads to reflection coefficients $\rho_s = -1$ and $\rho_o = +1$ for short and open circuit, respectively. They are opposite in phase but equal in magnitude. Hence, phase modulation occurs. The switch control signal is a periodic square wave signal of the period $1/f_{\text{mod}}$. When a signal with a frequency of f_{RF} inputs the switch, it gets mixed with the harmonics of the square wave. The modulated signal $f_{\text{RF}} \pm f_{\text{mod}}$ will reflect back and deliver the data toward the intended direction. This is the signal of interest that is maximized in this letter.

Manuscript received November 6, 2020; revised December 22, 2020; accepted January 3, 2021. Date of publication January 8, 2021; date of current version March 3, 2021. The work of Tauseef Ahmad Siddiqui was supported in part by the Aalto ELEC Doctoral School and in part by the University College of Engineering and Technology, The Islamia University of Bahawalpur, Bahawalpur, Pakistan. *(Corresponding author: Tauseef Ahmad Siddiqui.)*

The authors are with the Department of Electronics and Nanoengineering, School of Electrical Engineering, Aalto University, 02150 Espoo, Finland (e-mail: tauseef.siddiqui@aalto.fi; jari.holopainen@aalto.fi; ville.viikari@aalto.fi).

Digital Object Identifier 10.1109/LAWP.2021.3049972

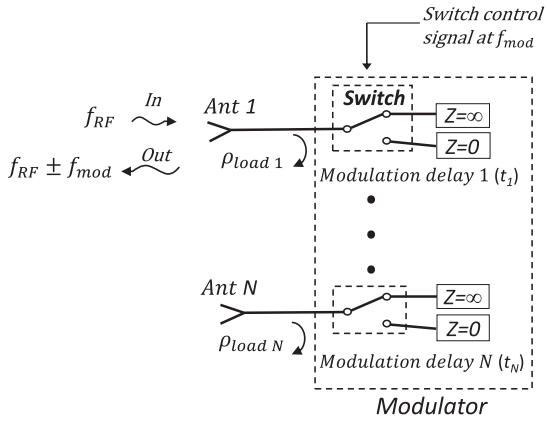

Fig. 1. Ideal switch switching between zero and infinite ohms load impedance.

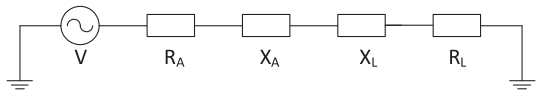

Fig. 2. Series model of a loaded antenna [16].

B. Modulation Effect

The switching of load impedances creates a modulation and the mixed modulated signal reflects back at the input of the switch. The modulated backscattered signal is proportional to the difference of the reflection coefficients $|\rho_s - \rho_o|$ of the two load impedances [13]–[15]. For ideal short and open circuit terminations, difference in the reflection coefficient $|\delta\rho| = |\rho_s - \rho_o| = 2$ but in real practice, $|\delta\rho|$ is less than 2. The equivalent series model of loaded antenna is illustrated in Fig. 2 to study the scattering effects. The antenna and load are expressed as impedances $Z_A = R_A + jX_A$ and $Z_L = R_L + jX_L$, respectively. The voltage V is the equivalent voltage generated by the incident wave. The RF current in the circuit can be calculated as [16]

$$I = \frac{V}{Z} = \frac{V}{(R_A + R_L) + j(X_A + X_L)} \tag{1}$$

where Z is the impedance of the circuit. Equation (1) consists of an incident voltage term multiplied by a mismatch term. The mismatch term can be expressed with the help of a reflection coefficient. Alternatively, considering the antenna array configuration, (1) in terms of the reflection coefficients at first harmonic assuming square-wave modulation, i.e., infinitely fast switching between the impedance states can be expressed as [16]

$$I_n = \frac{V_n}{R_A \pi}(\rho_s - \rho_o) \tag{2}$$

where I_n is the current in nth element, V_n is the incident voltage, R_A is the antenna resistance, and ρ_s and ρ_o are load impedance states. In (2), V_n carries the information of incident angle and can explicitly be written as

$$V_n = \underbrace{V_0 e^{-jkd(n-1)\cos\theta_i}}_{\text{Incident wave}} \tag{3}$$

where k is the wave number, d is the antenna element spacing, and θ_i is the incident angle.

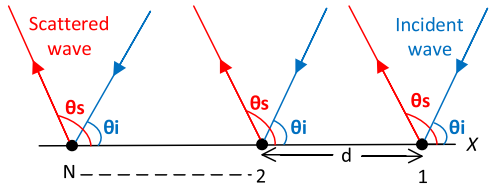

Fig. 3. Equally spaced linear array of isotropic point sources.

C. Modulation Delay

To create the phase difference between the outputs of the modulators, the switch control signals of these modulators are delayed in the time domain. This is done because a delay in the time domain creates a phase difference in the phasor domain. Equation (2) with modulation delay becomes

$$I_n = \frac{V_n}{R_A \pi}(\rho_s - \rho_o)\underbrace{(e^{-j\omega_{\text{mod}} t_n})}_{\text{Modulation delay}}\underbrace{(1 - e^{-j2\pi D})}_{\text{Duty cycle}} \tag{4}$$

in which $\omega_{\text{mod}} = 2\pi f_{\text{mod}}$, where $f_{\text{mod}} = 1/T$ is the modulation frequency, t_n is the time delay factor, and D represents the effect of duty cycle. The duty cycle of 50% maximizes the scattered power compared to other values of duty cycle. Hence, we use this value in our letter.

D. Array Factor

To study the scattering effects, consider an N-element of equally spaced linear array of isotropic point sources, as shown in Fig. 3. Also, consider the array to be retransmitting (scattering) an impinging electromagnetic wave. Now, the array factor in terms of scattered wave angle (θ_s) can be expressed as [17]

$$\text{AF} = \sum_{n=1}^{N} I_n \underbrace{e^{-jkd(n-1)\cos\theta_s}}_{\text{Scattered wave}}. \tag{5}$$

The mathematical expression of array factor in terms of incident wave, scattered wave, and modulation delay of antenna array can be written by combining (2)–(5) as

$$\text{AF} = \sum_{n=1}^{N} \underbrace{\frac{V_0}{\pi R_A}(\rho_s - \rho_o)}_{A_n} e^{-j(n-1)kd(\cos\theta_i + \cos\theta_s)} e^{-j\omega_{\text{mod}} t_n}. \tag{6}$$

The current for the nth element has magnitude (A_n) and affects the amplitude only and in our case, it remains constant for all elements. Hence, the general expression of array factor for N number of elements in transponder case is

$$\text{AF} = \frac{V_0}{\pi R_A}(\rho_s - \rho_o) \sum_{n=1}^{N} e^{-j(n-1)kd(\cos\theta_i + \cos\theta_s)} e^{-j\omega_{\text{mod}} t_n}. \tag{7}$$

The array factor is maximized and the main beam of the reflected wave can be steered in any direction irrespective of the incident angle by finding the optimal delays using (7). This is illustrated in Section III.

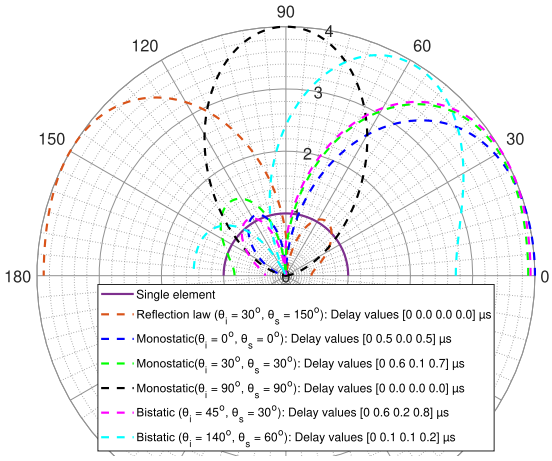

Fig. 4. Theoretical array factor magnitude using (7) for monostatic and bistatic cases with corresponding modulation delay values of four isotropic elements with quarter-wavelength spacing.

III. Beam Steerability With Optimal Delays

To illustrate the beam steering capability of the concept, the array factor magnitude, which can also be considered as an electric-field intensity, is plotted in MATLAB [18] using (7). Fig. 4 shows the amplitude of the scattered electric field under the assumptions of an ideal antenna array with omnidirectional antenna elements. The four-elements antenna array with interelement spacing of $d = \lambda/4$ is chosen and the modulation frequency f_{mod} is set to 1 MHz (i.e., signal of 1 μs time period). The reason for choosing this interelement spacing is due to the fact that grating lobes starts to appear in endfire array direction if more than $d = \lambda/2$ spacing is selected [17]. For the selection of f_{mod}, it should be large enough so that we can separate the useful information from the unmodulated wave. On the other hand, the modulation frequency should be small enough so that the modulated signal does not fall outside the system band. Additionally, the rise and fall time (23 ns) of RF switch limits f_{mod} to be smaller than 22 MHz. The delay value of first element is kept constant as reference and remaining three elements are time delayed with the resolution of 0.1 μs. The time delay resolution is a tradeoff between the measurement time and accuracy. We have chosen 0.1 μs time delay resolution, which leads to an acceptable number of measurements needed (1000 combinations of delay sets) and a reasonable phase resolution of the modulated signal (36°). According to our experience, 36° phase resolution provides a reasonable beam steering performance. It has been calculated using (7) and when the time resolution is 0.05 μs, the direction of the main beam may change up to 6°.

A. Monostatic Case

In monostatic case (retrodirectivity), the maximum reflection happens in the direction of incident wave when we have phase conjugation. The phases are conjugated for the corresponding symmetrically located elements in the array. For instance, in the case of four elements, the phase conjugation condition should be of the form $e^{j(-\pi)}$, $e^{j(-\pi/2)}$, $e^{j(\pi/2)}$, and $e^{j(\pi)}$. The modulation delay term in (7) is a periodic signal of the form $e^{-j\omega_{\text{mod}}t_n}$ (i.e., $e^{-j2\pi(\frac{t_n \pm nT}{T})}$) in which t_n is the time delaying factor. This time delay factor t_n is used for phase adjustment and we can always add (subtract) one period value (T) of 1 μs to fulfill the phase reverse condition for retrodirectivity. As illustrated in Fig. 4, when the incident angle is $\theta_i = 30°$, it reflects back at scattered angle $\theta_s = 30°$, when the delay values are [0 0.6 0.1 0.7] μs. These time delay values are in fact phase conjugated as [0 0.6 0.1 0.7] $-0.35 = [-0.35\ 0.25 - 1\ -0.25 + 1\ 0.35]$ μs $= [-0.35\ -0.75\ 0.75\ 0.35]$ μs, which corresponds to phase values of [$-126°$ $-270°$ $270°$ $126°$]. Similarly, in the case of endfire array, the optimal delay values [0 0.5 0.0 0.5] μs are phase conjugated as [-0.75,-0.25,0.25,0.75] μs. In broadside array case, when the optimal delays are uniform [0 0 0 0] μs, then the maximum radiation is perpendicular to the plane of array.

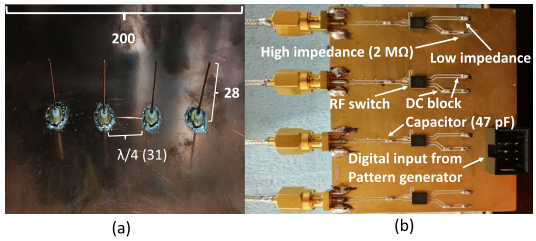

Fig. 5. (a) Manufactured antenna array with squared ground plane. (b) Modulators PCB circuit. All dimensions in millimeter.

B. Bistatic Case

In order to reflect the scattered wave at different angles, the delay values are optimized using (7). Fig. 4 shows multiple reflected beams in different directions with their corresponding optimal delay values. Any pair can be used for demonstration with the corresponding delay values. The results show how the beam of the scattered wave can be steered in any intended direction with the modulation delaying. When $\theta_i = 30°$ and there are no delays in the array elements, the beam scatters at $\theta_s = 150°$ exhibiting the reflection law property. Hence, for reflection law, no delays are optimal delays and angle of scattered wave is $\theta_s = 180° - \theta_i$.

IV. Measurements

A. Transponder Prototype

To validate the theoretical results, the transponder prototype is designed and measurement results are presented. Fig. 5 depicts the antenna array of four elements (monopoles) of transponder along with the modulator printed circuit board (PCB) circuit used in this letter. The modulator PCB is designed using PADS circuit designer. The single-pole double-throw RF switches (VSWA2-63DR+) are from minicircuits and lumped components are from Murata. The load impedances of the modulator PCB circuit are measured with the vector network analyzer and the difference in reflection coefficient $|\delta\rho| = |\rho_s - \rho_o|$ is around 1.3 (ideal value = 2) at the Wi-Fi frequency of 2.4 GHz.

B. Automated Measurement Setup

The measurements are performed in the anechoic chamber of Aalto University. It consists of a signal generator (R&S SMP 22), signal analyzer (R&S FSIQ 40), pattern generator

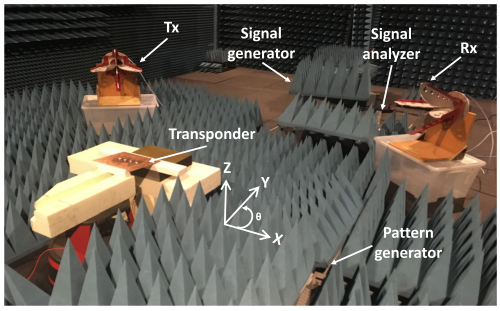

Fig. 6. Measurement setup used in the anechoic chamber for this letter. The distance (1.6 m) from the transponder to the Tx and Rx antennas is same to ensure the far-field conditions.

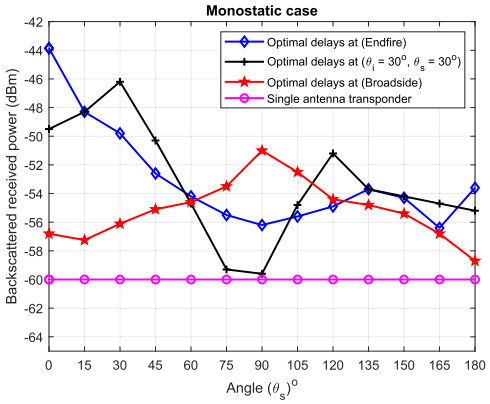

Fig. 7. Backscattered received power as a function of scattered angle with three different orientation angles by placing Tx and Rx at same location.

(Agilent 16720A-1), and transmitting (Tx) and receiving (Rx) antennas (ETS Lindgren 3164-08 quad-ridged horn antennas). The reader antenna (Tx) transmits the power of +24 dBm from the signal generator at 2.4 GHz. The transponder picks up this signal and backscatters a modulated signal that is received by the other reader antenna (Rx) and measured with the signal analyzer. The four channels of pattern generator are used to generate these user-defined patterns (delay sets) of digital logic high/low pulses. The measurement setup shown in Fig. 6 is automated with a PC running LabView virtual instrumentation to run these 1000 combinations of delay sets to find the optimal delay distribution at which the transponder would backscatter the maximum received power.

C. Measurement Results

To demonstrate the beam-steering capability of the studied transponder, the received signal strength is measured as a function of scattering angle by rotating the Rx antenna at different directions in the horizontal plane (*XY* plane). The backscattered received power is maximized by finding the optimal delay values from the 1000 combinations of delay sets in monostatic and bistatic cases. As seen in Fig. 7, when the optimal delay distribution is chosen, we see a clear maximum backscattered received power at endfire case (optimal delay values 0, 0.5, 0.1, 0.6 phase conjugated as -0.3, -0.8, 0.8, 0.3 μs), when θ_i and $\theta_s = 30^\circ$ (0, 0.2, 0.2, 0.4 phase conjugated as -0.7, -0.5,

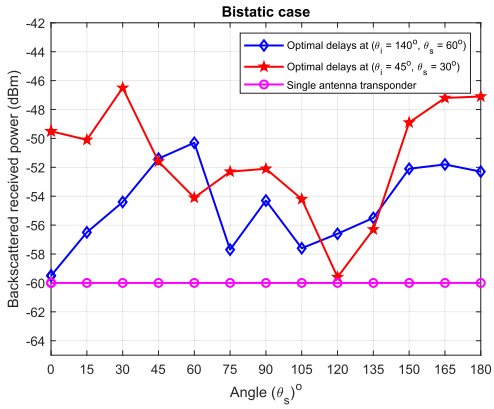

Fig. 8. Backscattered received power as a function of scattered angle with two different orientation angles by placing Tx and Rx at different location.

0.5, 0.7 μs) and broadside case (0, 0, 0, 0 μs). The received signal strength is measured in other directions as well with the same optimal delay values and the received power values are lower in those directions. The signal strength at endfire direction is 7 dB more as compared to broadside direction. Properly designed endfire array can avoid the backlobe and, therefore, provide higher gain than broadside array, whose main and back lobes are equally strong (assuming isotropic elements) [17]. In comparison with reference transponder, the enhancement in backscattered received power is up to 16.2 dB in endfire array direction. In bistatic case, any pair can be used for illustration. As shown in Fig. 8, the highest value of received power is measured when optimal delay values are used at that particular incident and scattered angle ($\theta_i = 45$, $\theta_s = 30$, [0, 0.3, 0.1, 0] μs and $\theta_i = 140$, $\theta_s = 60$, [0, 0, 0.9, 0.5] μs). In all these cases, the working principle of the prototype is the same, as illustrated in Fig. 4, with mathematical model. There is minimum scattering happening at 0°(blue curve) and 120°(red curve), the possible reason could be the nonoptimal phasing in that direction.

Due to nonidealities in measurements, the optimal delay values are not identical with theoretical cases. These include, for instance, the cables and connectors used to connect modulators with antennas introduce unknown reflections and time delays, which we have not currently accounted for in the theoretical model. Theory also neglects mutual coupling between the antennas and due to that embedded element patterns also differ from the individual ones. In antenna array theory, one of the main assumption is that the single element phase and radiation patterns are identical, which is not the case in practice. In the monostatic case, the transponder works as intended and the complex phase conjugated condition is demonstrated in theory as well as in measurements. In bistatic case, we see an increased side lobe level (around the angle of 150°), the possible reason could be the nonidealities in the measurement setup.

V. Conclusion

Despite being the first of its kind, the transponder has shown reasonably good results. The future work includes implementation of optimal delay distribution with microcontroller-based PCB with digital signal processing.

REFERENCES

[1] V. Liu, A. Parks, V. Talla, S. Gollakota, D. Wetherall, and J. R. Smith, "Ambient backscatter: Wireless communication out of thin air," in *Proc. ACM SIGCOMM*, Hong Kong, Aug. 2013, pp. 39–50.

[2] N. Van Huynh, D. T. Hoang, X. Lu, D. Niyato, P. Wang, and D. I. Kim, "Ambient backscatter communications: A contemporary survey," *IEEE Commun. Surveys Tuts.*, vol. 20, no. 4, pp. 2889–2922, Oct.–Dec. 2018.

[3] C. Yang, J. Gummeson, and A. Sample, "Riding the airways: Ultra-wideband ambient backscatter via commercial broadcast systems," in *Proc. IEEE Conf. Comput. Commun.*, Atlanta, GA, USA, May 2017, pp. 1–9.

[4] L. C. Van Atta, "Electromagnetic reflector," U.S. Patent 2 908 00 2, Oct. 6, 1959.

[5] C. Pon, "Retrodirective array using the heterodyne technique," *IEEE Trans. Antennas Propag.*, vol. AP-12, no. 2, pp. 176–180, Mar. 1964.

[6] M. S. Trotter, C. R. Valenta, G. A. Koo, B. R. Marshall, and G. D. Durgin, "Multi-antenna techniques for enabling passive RFID tags and sensors at microwave frequencies," in *Proc. IEEE Int. Conf. RFID*, Apr. 2012, pp. 1–7.

[7] G. Koo, "Signal constellations of a retrodirective array phase modulator," Master's thesis, School Elect. Comput. Eng., Georgia Inst. Technol., Atlanta, GA, USA, 2011.

[8] M. M. Islam, K. Rasilainen, S. K. Karki, and V. Viikari, "Designing a passive retrodirective wireless sensor," *IEEE Antennas Wireless Propag. Lett.*, vol. 16, pp. 1739–1742, 2017.

[9] M. Alhassoun, M. A. Varner, and G. D. Durgin, "Theory and design of a retrodirective rat-race-based RFID tag," *IEEE J. Radio Freq. Identification*, vol. 3, no. 1, pp. 25–34, Mar. 2019.

[10] T. A. Siddiqui, J. Holopainen, and V. Viikari, "Ambient backscattering transponder with independently switchable Rx and Tx antennas," *IEEE Sensors Lett.*, vol. 3, no. 5, May. 2019, Art no. 3500704.

[11] V. Mangal, G. Atzeni, and P. R. Kinget, "Multi-antenna directional backscatter tags," in *Proc. 48th Eur. Microw. Conf.*, Sep. 2018, pp. 25–27.

[12] T. A. Siddiqui, P. Khanal, J. Holopainen, and V. Viikarii, "Concept of beam steerable transponder based on load modulation," in *Proc. 14th Eur. Conf. Antennas Propag*., Copenhagen, Denmark, Mar. 2020.

[13] T. A. Siddiqui, P. Khanal, J. Holopainen, and V. Viikari, "Broadband transponder based on frequency-reconfigurable cluster antenna and phased modulators," *IEEE Antennas Wireless Propag. Lett.*, vol. 9, no. 2, pp. 238–242, Feb. 2020.

[14] T. A. Siddiqui, P. Khanal, J. Holopainen, and V. Viikari, "Further investigations on frequency-reconfigurable transponder based on mutually coupled antenna cluster and phased modulators," *URSI Radio Sci. Lett.*, Oct. 2020.

[15] J. X. Yun and R. G. Vaughan, "A view of the input reflection coefficient of the N-port network model for MIMO antennas," in *Proc. IEEE Int. Symp. Antennas Propag.*, Jul. 2011, pp. 297–300.

[16] P. Pursula, "Analysis and design of UHF and millimetre wave radio frequency identification," Ph.D. dissertation, Helsinki Univ. Technol., VTT Technical Research Centre of Finland, Espoo, Jan. 2009.

[17] W. L. Stutzman and G. A. Thiele, "Array antennas," in *Antenna Theory and Design*, 3rd ed. Hoboken, NJ, USA: Wiley, 2012, pp. 271–336, ch. 8.

[18] MathWorks, MatlabR2020b, Jul. 20, 2020. [Online]. Available: https://se.mathworks.com/products/matlab.html